Desalination and Water Treatment
www.deswater.com

doi: 10.5004/dwt.2017.21244

96 (2017) 61–68
November

Influence of the magnetizing pretreatment on the mitigation of membrane scaling during nanofiltration

Cong Ma[a,b], Dongliang Liu[a], Liang Wang[a,*], Zhaohui Zhang[a], Hongwei Zhang[a]

[a]*State Key Laboratory of Separation Membranes and Membrane Processes, School of Environmental and Chemical Engineering, Tianjin Polytechnic University, Tianjin 300387, China, Tel. +86 22 83955392; email: mashi7822@163.com (L. Wang), Tel. +86 22 83955883; email: macong_0805@126.com (C. Ma), Tel. +86 13012251021; email: 13012251021@163.com (D.L. Liu), Tel. +86 22 83955163; email: zzh7448@126.com (Z.H. Zhang), Tel. +86 22 83955666; email: hwzhang@tju.edu.cn (H.W. Zhang)*
[b]*Department of Chemical and Biomolecular Engineering, University of Connecticut, 191 Auditorium Road Unit 3222, Storrs, CT 06269-3222, USA*

Received 3 March 2017; Accepted 18 July 2017

ABSTRACT

One of the major limitations of the application of nanofiltration (NF) membrane processes in desalination of brackish water or seawater is inorganic fouling, which could be named as scaling and the membrane scaling issues could reduce the efficiencies of membrane separation process and membrane lifetime. This research focused on the main factors mitigating inorganic membrane fouling during NF process via a magnetizing pretreatment. The magnetization device constructs a high gradient magnetic field with an external neodymium ferrum boron permanent magnet and an internal stainless steel wool, which could generate a magnetic field through magnetization. Various factors involved in the magnetization process such as time, $CaCO_3$ concentration, temperature, and steel wool packing rate (the area ratio of steel wool to the effective inner surface of the magnetization device) were studied over a flat sheet NF membrane from Vontron. All these factors affected the magnetizing pretreatment, the efficiency of which was followed by the transformation of calcite into aragonite. As revealed by the flux variation, the inorganic fouling reduction reached a maximum with the magnetization time (4 h in this study). The fouling tests carried out by increasing $CaCO_3$ concentration and steel wool packing rate resulted in the formation of a thick and dense cake layer that induced membrane fouling increment and membrane flux decline. Additionally, the inorganic fouling was correlated with temperature. In this study, the optimal operating conditions were determined to control membrane fouling at 4 h of magnetizing time (3 mmol/L of $CaCO_3$, 20°C and 5% of steel wool packing rate), 35°C (3 h of magnetizing time, 6 mmol/L of $CaCO_3$ and 15% of packing rate), and 10% of steel wool packing rate (2 h of magnetizing time, 1 mmol/L of $CaCO_3$ and 35°C) with a magnetizing pretreatment for 3 mmol/L of $CaCO_3$ (4 h of magnetizing time, 30°C and 10% of steel wool packing rate). Scanning electron microscopy (SEM) was used to investigate membrane fouling during NF process. Unlike calcite that formed a thick and dense layer, these observations demonstrated that aragonite $CaCO_3$ precipitated as a thin and loose cake layer with good permeability.

Keywords: Magnetizing pretreatment; Inorganic scaling fouling; NF; Calcite; Aragonite; Influence factors

* Corresponding author.

Presented at the 9th International Conference on Challenges in Environmental Science & Engineering (CESE-2016), 6–10 November 2016, Kaohsiung, Taiwan.

1. Introduction

As a result of severe freshwater shortages, numerous advanced technologies for water purification including desalination of brackish water or seawater have emerged to secure clean water supply [1,2]. In the case of water desalination, the focus remained on nanofiltration (NF) and reverse osmosis (RO) membranes as feasible approaches to high-quality clean water production. NF membranes are more promising for the production of low-cost drinking water because of their lower operational pressures, higher flux, and higher selectivity characteristics compared with RO membranes [3–7].

However, soluble salts in the feed stream tend to precipitate on the membrane surface during desalination of brackish water and seawater (i.e., salt scaling) negatively affecting the desalination process in terms of efficiency and membrane lifetime. Because they reduce the permeate flux and induce the physical damage of membrane due to membrane scaling [8–11]. Therefore, membrane scaling should be alleviated to prolong the service lifetime of the membrane [12]. With the aim to improve the practical application of membranes, research on membrane scaling has become increasingly important.

Calcium carbonate is the most common scaling salt generated during water purification by NF. In order to solve this problem, many physicochemical treatment techniques have been used including utilization of acids [13], scale inhibitors [14,15], ion-exchange materials [16], and magnetic [17] or electrostatic [18] fields. Particularly, scaling prevention via magnetic water treatment has a long history of practical application because of its convenient application and less investment.

Previous studies have reported that scaling deposition proceeds in two steps (i.e., nucleation and crystal growth). The magnetic field was reported to affect the calcium carbonate polymorphs (i.e., calcite and aragonite) formed by the constant composition method [19–21] as well as the crystal morphology that varied with the phase formed (i.e., calcite or aragonite) [22,23]. Li et al. [9] reported that the scaling layer of deposited $CaCO_3$ obtained under non-magnetizing conditions was denser and thicker compared with that obtained in the presence of a magnetic field (0.2 T). Additionally, this magnetic field favored the formation of crystal aragonite vs. calcite which was suppressed. The NF membrane scaling performance during unstirred dead-end filtration was discussed while varying the intensity of the magnetic field [24].

Furthermore, the magnetizing effects were found to be affected by the nature of the solution and the operating conditions including pH [25], the impurity ion [26,27], the magnetic intensity [19,21], operating condition [28] and the magnetic substance employed [29]. All $CaCO_3$ crystallization in the above researches was either in the permanent magnetic field or in the variable magnetic field, but out of high magnetic field gradient. Schulze and Dixon [30] found that the high magnetic field gradients could be supplied by a filter of ferromagnetic stainless steel wool placed in a strong magnetic field. Long et al. [24] studied the relationship between the NF membrane flux and $CaCO_3$ crystallization in the unstirred dead-end NF process in the presence of the magnetic field. However, most NF membranes were applied in the cross-flow process in practice. Furthermore, few studies were found to report the effect of the chemical properties of the solution on the $CaCO_3$ crystallization upon magnetic treatment in magnetic field with high gradient in NF process. Thus, in this study, the high magnetic field gradient (supplied by the steel wool) was applied in the magnetizing pretreatment for NF process by the cross-flow mode.

In this study, the efficiency of the magnetizing treatment (high magnetic field gradient) for avoiding membrane fouling was investigated by following the changes of the solution properties (i.e., $CaCO_3$ concentration and temperature), the magnetizing time, and the steel wool packing rate. The normalized permeate flux was determined to assess membrane fouling. Scanning electron microscopy (SEM) and X-ray diffraction (XRD) analyses were utilized to investigate the precipitation of $CaCO_3$ on the membrane surface and its crystal morphology.

2. Materials and methods

2.1. Materials

All chemicals and reagents used in this study were of analytical grade. Milli-Q water was used for the preparation of all working solutions. In the solution, the $CaCl_2$ and Na_2CO_3 solutions were mixed in these experiments to prepare $CaCO_3$ solution. The scaling experiments were carried out with different concentration $CaCO_3$ solution (3, 6, and 9 mmol/L) and the solution pH was 9.75 ± 0.05. This method has been applied in the quantitative study of $CaCO_3$ deposition on NF membranes via ultrasonic time-domain reflectometry [9].

The NF membranes (VNF1-1812) were purchased from Vontron (Guiyang province, China), and their properties are summarized in Table 1. A self-regulating flat-sheet membrane module with an NF membrane diameter of 55 mm was used. The magnetizing apparatus was composed of permanent magnets in the outside and stainless steel wool (50 μm in diameter) in the inside. The steel wool was magnetized by permanent magnets so that it self-generates a magnetic field. The self-generated magnetic field formed a high magnetic field gradient in the magnetizing apparatus. The intensity of magnetic field was approximately 0.3–0.4 T. The experimental pipes were all made of PVC (8 mm in diameter).

2.2. Experimental procedure and conditions

As shown in Fig. 1, the experimental process was divided into two parts separately: (i) the magnetizing (or non-magnetizing) pretreatment and (ii) the cross-flow NF membrane filtration process. The experimental procedure can be described in detail as follows: the magnetizing

Table 1
Properties of NF membrane

Module type	VNF1-1812
Module configuration	Spiral wound
Membrane effective area (m^2)	0.41
Feed temperature (°C)	<45
Range of feed pH	3–10
Operational pressure (MPa)	<2.07

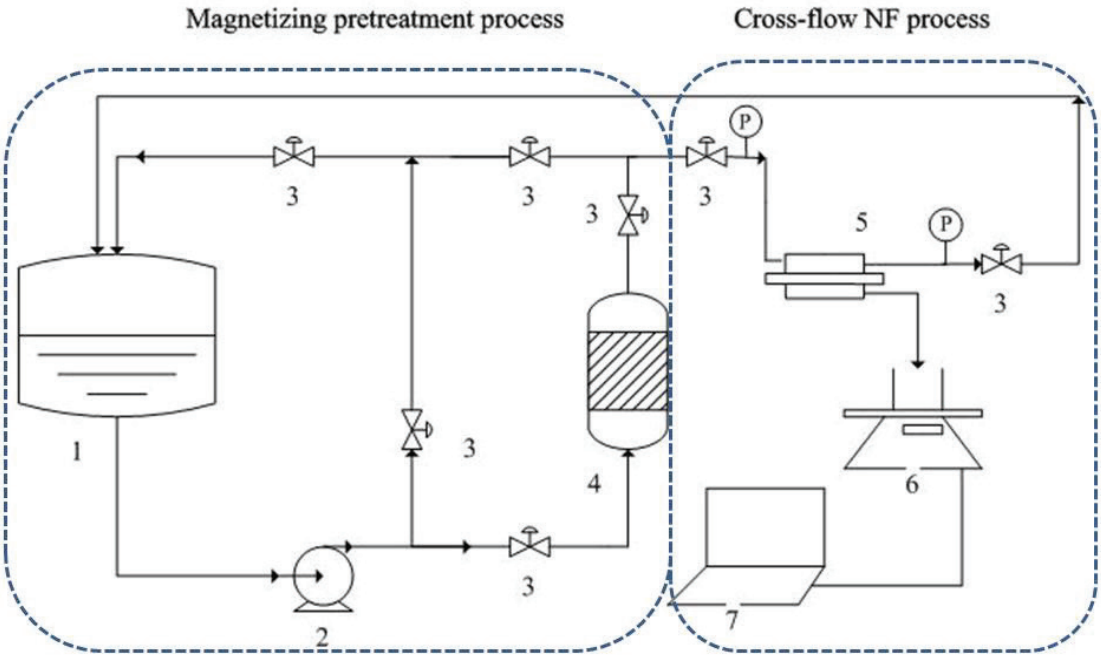

Fig. 1. Schematic diagram of experimental process. (1) Feeding tank; (2) diaphragm pump; (3) valve; (4) magnetic apparatus; (5) flat-sheet membrane module; (6) balance; (7) PC.

apparatus was set to one outlet pipe of a diaphragm pump, the effluent water samples subsequently entered into the feeding tank, and finally cycled (cycling flow rate: 0.05 m/s) in the pipes to magnetize the solution. After some cycle time, the solution was conducted to the NF cross-flow filtration process (operation time: 480 min; operation pressure: 0.8 MPa). The membrane was soaked in pure water for at least 8 h before the experiment. Each experiment started with pure water being circulated through the system for 1 h at the same conditions as the scaling experiment. As for the control experiment, non-magnetizing solutions were placed in another pipe out of the magnetic apparatus. During the filtration, the permeate volume was measured every 30 min by an automatic data-logging balance device connected with a computer.

The effect of a single variable on the membrane scaling process was studied by maintaining the rest of factors constant. The scaling experiments were carried out by varying different parameters such as the magnetizing time (0, 1, 2, and 4 h), the $CaCO_3$ concentration (3, 6, and 9 mmol/L), the temperature (20°C, 30°C, and 35°C), and the steel wool packing rate (5%, 10%, and 15%).

The fouled NF membranes were removed from the module after each operation, subsequently rinsed with deionized water, and their integrity inspected before drying them in the desiccator for surface analysis.

2.3. Analytical methods

The normalized permeate flux (Q) was determined to study the properties of the NF membrane after being fouled at different conditions. Low membrane fouling extents correspond to higher Q values. Q was calculated as follows:

$$Q = \frac{J_T}{J_0} \times 100\% \quad (1)$$

where J_T and J_0 are the temporal and initial fluxes, respectively.

Additionally, field emission scanning electron microscopy (S-4800, Japan) was used to examine the morphology of the scaling inorganic $CaCO_3$ deposited on the NF membrane surface. The crystal phase compositions of $CaCO_3$ were determined by XRD (D/MAX-2500X, Japan). In our previous studies, the morphology and crystal compositions of $CaCO_3$ were studied by SEM and XRD, respectively, and calcite and aragonite phases were detected and compared with previous works. The qualitative analysis of the XRD patterns was in good agreement with previous results [31]. Thus, the acicular crystal $CaCO_3$ phase was identified as aragonite while cubic crystal $CaCO_3$ corresponded to calcite (Fig. 2). This morphological analysis of the fouled membrane was required to establish a correlation between the water flux and the fouling layer.

3. Results and discussion

3.1. Effect of the magnetizing time on the inorganic membrane fouling of NF process

Membrane fouling was minimized at a critical magnetizing time. As shown in Fig. 3(A), the magnetizing time greatly affected the membrane flux. Thus, membrane fouling was alleviated under magnetizing conditions. Thus, Q gradually increased with the magnetizing time up to 4. These results indicated that 4 h is the optimal magnetizing time to mitigate membrane scaling in this study.

The inorganic scaling was built up on the membrane surface thereby reducing the water flux [24,32,33]. When the

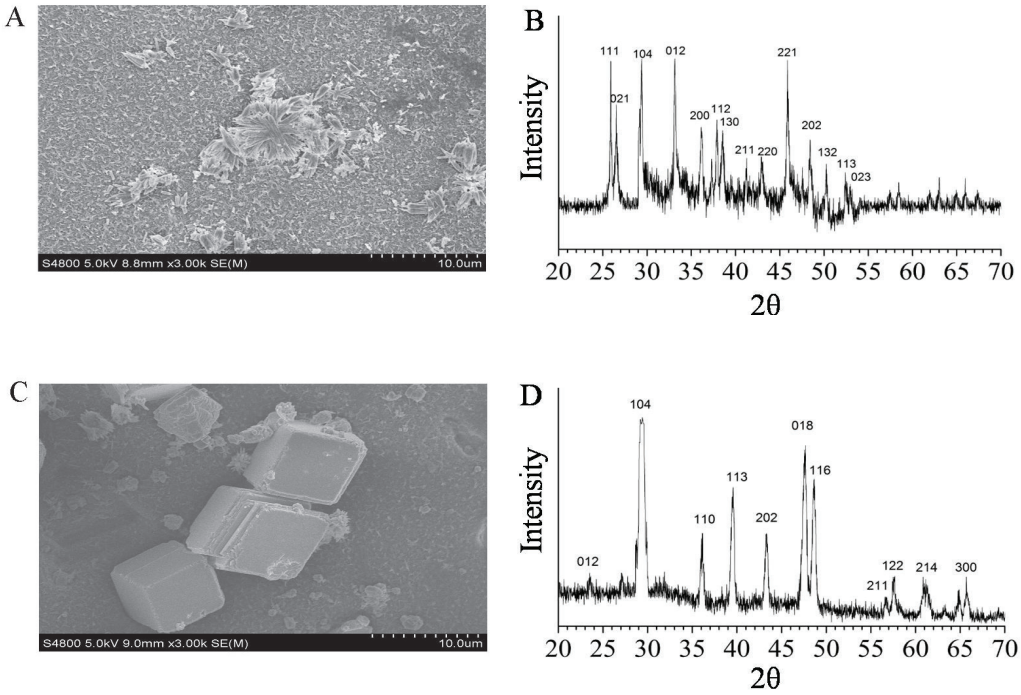

Fig. 2. XRD patterns and SEM images of $CaCO_3$ crystal.

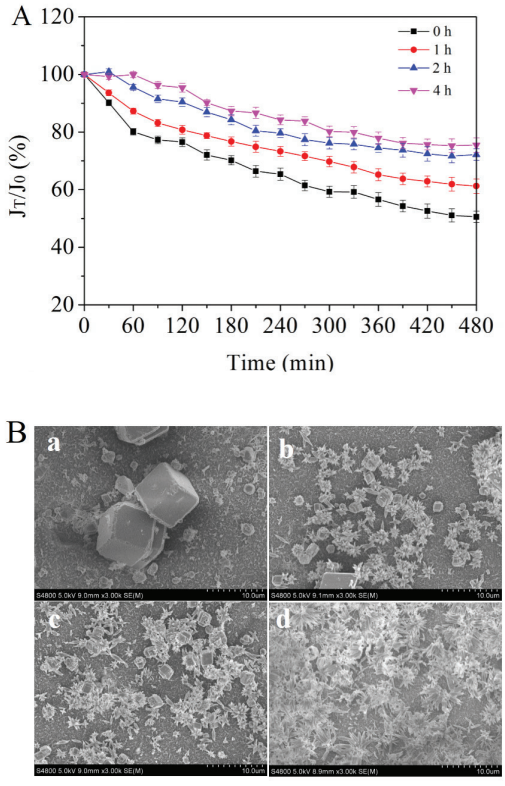

Fig. 3. Effect of the magnetizing time on inorganic membrane fouling of NF process (3 mmol/L of $CaCO_3$, 20°C and 5% of steel wool packing rate). (A) Normalized permeate flux curves of NF membranes; (B) SEM images of NF membranes with different magnetic times (a, 0 h; b, 1 h; c, 2 h; d, 4 h).

magnetizing time reached 4 h, the permeate flux reduction was less than half that obtained under non-magnetizing conditions (decreased by 25%; Fig. 3(A)). These results can be explained by a lower $CaCO_3$ precipitation on the membrane surface under magnetizing conditions.

In the NF process, the crystals are formed only when the supersaturation (S) on the membrane surface is higher than 1 [24]. The supersaturation can be calculated by Eq. (2).

$$S = \frac{c_m}{c_s} \tag{2}$$

where c_m and c_s are the concentrations on the membrane surface and saturated concentration of the solute, respectively.

The cake layer played a dominant role on the NF membrane inorganic scaling process [34,35]. SEM investigations were carried out to investigate the effects of the magnetizing pretreatment over the $CaCO_3$ solution at different magnetizing times (Fig. 3(B)). The crystal morphology of $CaCO_3$ on the membrane surface shifted from crystal cubic calcite to acicular aragonite crystal phase with the magnetizing time. The number of aragonite crystals gradually increased at the expense of calcite which completely disappeared at magnetizing time of 4 h. This was attributed to the magnetic field changing the crystal morphology from calcite to aragonite and promoting the growth of aragonite crystals [21]. Longer magnetizing times favored conversion and growth rate. Similar results (i.e., nucleation of calcite being prevented by the magnetic field) were reported by Chibowski et al. [29] and Gabrielli et al. [36]. With regard to the growth behavior, calcite nearly stopped its growing whereas aragonite started to grow at longer magnetizing times [19,21]. This can be explained by the secondary nucleation theory proposed by Bauer [37] and Tai et al. [38]. According to these researchers,

a secondary nucleation is carried out by an adsorption layer composed of solute clusters on the surface of growing seed crystals, awaiting incorporation into the growing seed crystals. The magnetic force is likely to alter the structure of the adsorbed solute clusters upon the magnetizing pretreatment. Subsequently, the adsorption layers are desorbed from the crystal interface once they become unfavorable to form calcite crystals. Longer magnetizing times strengthen the effect of this magnetic force. Thus, as shown in Fig. 3((B), inset d), a higher number of aragonite crystals were formed at the expense of calcite.

It is interesting to note that both the deposition on the membrane surface and the permeate flux were maximized at 4 h of magnetizing time. The similar result has been concluded by Long et al. [24]. The acicular structure of small aragonite did not deposit closely to the membrane surface, there was some gap space during the aragonite–aragonite and aragonite membrane surface. As a result, the formed cake layer on the membrane surface was thin, loose and porous, therefore showed good permeability with the decreased of the concentration polarization. In contrast, due to the special cubic structure, the first layer of larger calcite crystals stuck closely to membrane surface, covering certain membrane pore, and then resulted in a thick and dense cake layer with poor permeability. Since this dense cake layer was transformed into a loose cake layer for magnetizing times ranging from 1 to 4 h, the water flux was maximum at 4 h magnetizing time. We believe that the different efficiency of the crystal morphology conversion during the permanent magnetic field was produced by the different operation conditions.

3.2. Effect of the calcium carbonate concentration on the inorganic membrane fouling of NF process

This experiment was carried out at a magnetizing time of 4 h. The normalized permeate flux values as a function of the filtration time are summarized in Fig. 4(A). The fouling experiments were carried out with varying concentrations (3–9 mmol/L) of $CaCO_3$ during pre-magnetic filtration (PMF). As can be seen in Fig. 4(A), the permeate water decreased as scaling proceeded for each $CaCO_3$ concentration. This may be produced by the gradual formation of the cake layer at the initial stage, and this cake layer resulted in a stable flux [39]. Higher concentrations of $CaCO_3$ resulted in more serious membrane fouling because of larger $CaCO_3$ precipitate accumulation.

Furthermore, as shown in Fig. 4(A), more pronounced flux decreases were obtained with high $CaCO_3$ concentrations during PMF. At these conditions, the precipitate was formed faster and to a larger extent on the membrane surface forming a thicker cake layer. Similar results were obtained by Li et al. [9], who used ultrasonic time-domain reflectometry to quantify the precipitation and growth of $CaCO_3$ scaling on the surface of NF membranes at different concentrations of $CaCO_3$ under a magnetic field. The normalized permeate flux increased by 10% after 420 min of magnetizing pretreatment for a 3 mmol/L $CaCO_3$ solution. According to Chen et al. [40] and Dawe and Zhang [41], the formation of the different polymorphs of $CaCO_3$ depends on the concentration of $CaCO_3$. Thus, calcite was favored at high concentrations, with the crystal growth rate increasing with the $CaCO_3$

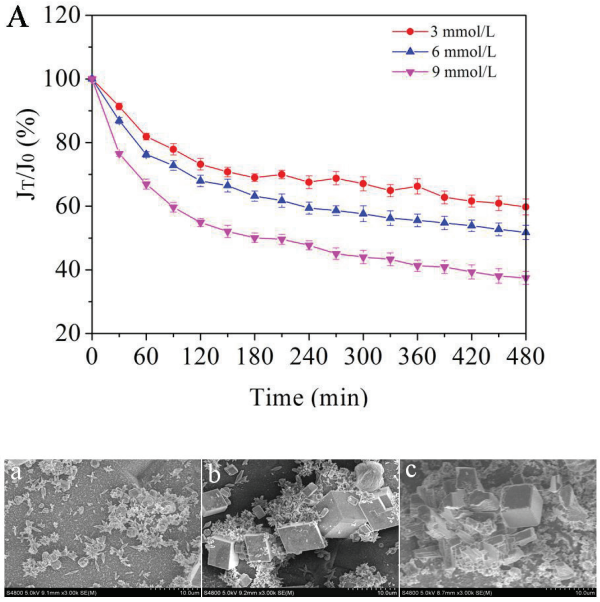

Fig. 4. Effect of the calcium carbonate concentration on inorganic membrane fouling of NF process (4 h of magnetizing time, 30°C and 10% of steel wool packing rate). (A) Normalized permeate flux decline curves of NF membranes. (B) SEM images of NF membrane using magnetizing pretreatment with different concentrations (a, 3 mmol/L; b, 6 mmol/L; c, 9 mmol/L).

concentration. The supersaturation ratio (S) was proposed to express the scaling tendency by Chen et al. [40]. S is calculated as the ratio of the activity of a given ion (i.e., Ca^{2+} and CO_3^{2-}) to the solubility product (K_{sp}) of $CaCO_3$. The activity of the ion is closely (and positively) related to the $CaCO_3$ concentration. Therefore, higher $CaCO_3$ concentrations tend to promote crystal formation. Thus, the efficiency for the transformation from calcite to crystal aragonite phase was reduced because of larger amounts of calcite crystals being formed at high $CaCO_3$ concentrations as a result of the magnetizing pretreatment after some magnetizing time.

Fig. 4(B) shows the SEM images of some $CaCO_3$ crystal formed on the membrane surface at different concentrations upon a magnetizing pretreatment. The SEM photographs of the structures formed revealed the presence of larger amounts of calcite crystal phase at higher $CaCO_3$ concentrations. The aragonite crystals formed a thin and loose cake layer with good permeability at low concentrations. On the other hand, the cake layer comprised calcite crystals was thick and dense. This result can be explained by two effects. First, larger amounts of the precipitate were formed on the membrane surface at higher concentrations of $CaCO_3$ to form a thicker cake. Second, the $CaCO_3$ crystal phase was not completely transformed from calcite to aragonite by the magnetic field since a large amount of calcite precipitated (Figs. 4(B) insets b and c), and the subsequent deposit formed on the membrane was dense. This is consistent with the results by Her et al. [42] reporting that a heterogeneous crystallization (i.e., aragonite and calcite) resulted in a more significant flux decline compared with homogeneous crystallization (i.e., aragonite). Based on the above result, the amount of calcite and aragonite increased with the $CaCO_3$ concentration on

the NF membrane surface upon magnetizing pretreatment. However, the operation conditions (i.e., magnetizing time and temperature) can alter the formation of $CaCO_3$ crystals, which is beneficial to mitigate membrane fouling.

3.3. Effect of the temperature on the inorganic membrane fouling of NF process

Fig. 5(A) shows the normalized water flux while varying the temperature from 20°C to 35°C during PMF. Water flux first sharply decreased at the beginning of the operation and gradually attenuated with time to finally level off. Lower temperatures led to faster flux declines. Thus, the permeate flux decreased by 45% and 38% during PMF at temperatures of 20°C and 35°C, respectively. This result may be attributed to larger amounts of precipitate depositing on the membrane surface, this leading to poorer permeability of the cake layer at lower temperatures.

SEM was used to analyze the surface structure of the NF membranes after the PMF experiments (Fig. 5(B)). Remarkably, the amount and size of precipitable aragonite increased with the temperature and the calcite gradually disappeared. Similar results reported a synergetic effect of the magnetic field and the temperature on the aragonite growth, thereby accelerating the transformation from calcite into aragonite crystal phase [43]. The proposed transformation mechanism under a magnetic field is related with the formation of different $CaCO_3$ clusters existing in the supersaturated solution [19]. This mechanism assumes that the calcite clusters transform into aragonite by the Lorentz force upon magnetization of the supersaturated solution. A larger number of clusters are beneficial to aragonite growth since it produces a higher surface integration rate at higher temperatures. Previous studies have also

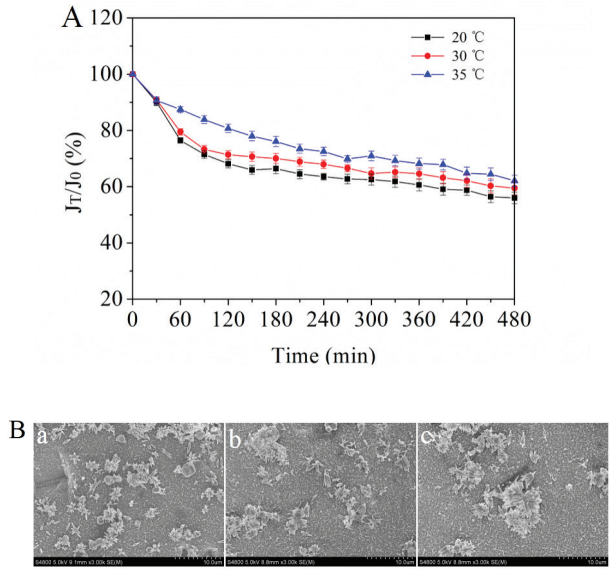

Fig. 5. Effect of the temperature on inorganic membrane fouling of NF process (3 h of magnetizing time, 6 mmol/L of $CaCO_3$ and 15% of packing rate). (A) Normalized permeate flux curves of NF membranes; (B) SEM images of NF with different temperatures (a, 20°C; b, 30°C; c, 35°C).

reported the effect of temperature on the crystal structure of $CaCO_3$ on tube walls [44]. They concluded that high temperature accelerates the crystallization transformation from calcite to aragonite under magnetic field conditions. The needle aragonite precipitate was stacked on the membrane surface, which reduced flux decline as a result of good permeability. Thus, the magnetizing pretreatment can mitigate membrane fouling at an appropriate temperature promoting complete calcite transformation into aragonite during the magnetizing process. The effect of the temperature on the crystal morphology of $CaCO_3$ was closely related to the solution concentration, the magnetic field intensity, and other operation conditions.

3.4. Effect of the steel wool packing rate on the inorganic membrane fouling of NF process

Steel wool was magnetized such that it self-generated a magnetic field. Thus, the primary uniform magnetic field distribution was changed into a magnetic field gradient. The magnetic force was applied to the solute that cut the magnetic induction line. The higher gradient magnetic field might generate greater magnetic force.

Lower packing rates generated lower ranges of high gradient magnetic field, and the superabundant steel wools caused magnetic short circuits by touching each other (reducing magnetic force). Thus, the effective space of the magnetic field was reduced. To compare the effectiveness of the packing rate, the experiments were conducted at packing rates of 5%, 10%, and 15%. As illustrated in Fig. 6(A), the permeate flux decreased by 43.2%, 30.6%, and 37.7% at 5%, 10%, and 15% packing rates, respectively. Thus, a reasonable packing rate (10%) improved the magnetic field gradient and alleviated membrane fouling. Previous studies have reported lower calcite growth rates and dense cake layer formation on the membrane surface compared with aragonite deposits at high magnetic intensities [19].

Fig. 6(B) shows the SEM micrographs of the magnetically pretreated precipitates on the membrane surface. Lower amount of homogeneous crystallization (i.e., aragonite) at a packing rate of 10% compared with heterogeneous crystallization (i.e., aragonite and calcite) at a packing rate of 5% and 10% was found obviously in Fig. 6(B). This finding was consistent to the membrane flux decline (Fig. 6(A)) [42]. The proposed mechanism for the formation of aragonite in the presence of magnetic field was explained in terms of a significantly stiffer ground electronic state of aragonite compared with calcite. Thus, in order to form aragonite instead of calcite, Ca^{2+} and CO_3^{2-} ions would require higher kinetic energies to overcome the repulsive forces of potential barrier [22]. Under a magnetic field, the charged species (Ca^{2+} and CO_3^{2-}) obtain the required kinetic energy via magnetohydrodynamic processes involving Lorenz forces [29,31]. High gradient magnetic fields can enhance the function of the Lorenz forces. Thus, the kinetic energy required to achieve the ground state of the aragonite could be provided by filling 10% of steel wools under a magnetic field. The aragonite cake layer is thin and loose and shows good permeability. The low hydraulic resistance of the aragonite precipitate is responsible for the good flux permeability observed for this

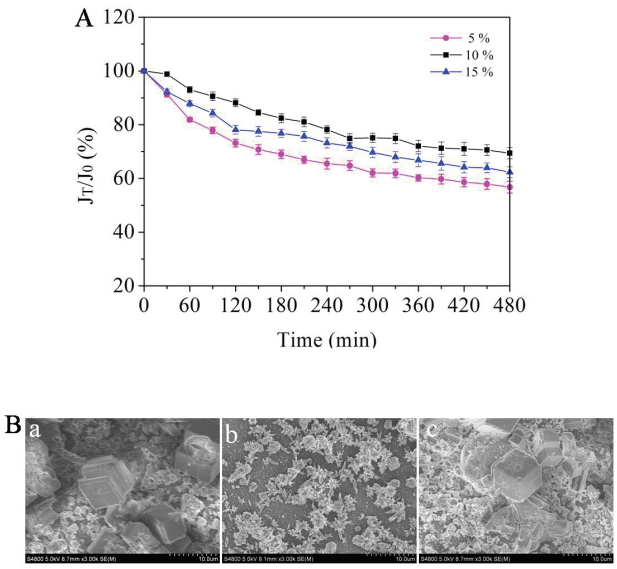

Fig. 6. Effect of the steel wool packing rate on inorganic membrane fouling of NF process (2 h of magnetizing time, 1 mmol/L of $CaCO_3$ and 35°C). (A) Normalized flux decline curves of NF membranes; (B) SEM images of NF membranes using magnetic pretreatment with different steel wool packing rates (a, 5%; b, 10%; c, 15%).

material [45]. Thus, 10% is an optimal packing rate to mitigate membrane scaling under magnetic field conditions.

4. Conclusions

The magnetizing pretreatment (high magnetic field gradient) was investigated herein with the aim to maximize the effect of magnetization on NF membrane fouling mitigation. The results showed that the optimum operational parameters for the magnetizing pretreatment were influenced by the concentration of $CaCO_3$. Thus, higher $CaCO_3$ concentration resulted in larger amounts of precipitated $CaCO_3$ crystals. In this study, the optimum operational parameters mitigating membrane fouling were 4 h of magnetizing time (3 mmol/L of $CaCO_3$, 20°C and 5% of steel wool packing rate), 35°C (3 h of magnetizing time, 6 mmol/L of $CaCO_3$ and 15% of packing rate), and 10% of steel wool packing rate (2 h of magnetizing time, 1 mmol/L of $CaCO_3$ and 35°C) with a magnetizing pretreatment for 3 mmol/L of $CaCO_3$ (4 h of magnetizing time, 30°C and 10% of steel wool packing rate). These operation conditions promoted the transformation of calcite into aragonite, the latter of which was characterized by small acicular crystals forming a thin and loose cake layer on the membrane surface with good permeability. On the other hand, the larger cubic calcite crystals generated a thick and dense cake layer with poor permeability.

Acknowledgments

The authors gratefully acknowledge financial support provided by the National Science Foundation of China (No. 51508383, 51478314, and 51638011) and the State Key Laboratory of Separation Membranes and Membrane Processes (No. 15PTSYJC00230 and 15PTSYJC00240).

References

[1] R. Valladares Linares, Z. Li, V. Yangali-Quintanilla, N. Ghaffour, G. Amy, T. Leiknes, J.S. Vrouwenvelder, Life cycle cost of a hybrid forward osmosis – low pressure reverse osmosis system for seawater desalination and wastewater recovery, Water Res., 88 (2016) 225–234.
[2] Y. Lu, I.M. Abu-Reesh, Z. He, Treatment and desalination of domestic wastewater for water reuse in a four-chamber microbial desalination cell, Environ. Sci. Pollut. Res. Int., 23 (2016) 17236–17245.
[3] G. Mustafa, K. Wyns, P. Vandezande, A. Buekenhoudt, V. Meynen, Novel grafting method efficiently decreases irreversible fouling of ceramic nanofiltration membranes, J. Membr. Sci., 470 (2014) 369–377.
[4] W. Jiang, Y. Wei, X. Gao, C. Gao, Y. Wang, An innovative backwash cleaning technique for NF membrane in groundwater desalination: fouling reversibility and cleaning without chemical detergent, Desalination, 359 (2015) 26–36.
[5] C. Quist-Jensen, F. Macedonio, E. Drioli, Integrated membrane desalination systems with membrane crystallization units for resource recovery: a new approach for mining from the sea, Crystals, 6 (2016) 1–13.
[6] D. Dolar, T. Ignjatic Zokic, K. Kosutic, D. Asperger, D. Mutavdzic Pavlovic, RO/NF membrane treatment of veterinary pharmaceutical wastewater: comparison of results obtained on a laboratory and a pilot scale, Environ. Sci. Pollut. Res. Int., 19 (2012) 1033–1042.
[7] N. Kasim, A.W. Mohammad, S.R.S. Abdullah, Characterization of hydrophilic nanofiltration and ultrafiltration membranes for groundwater treatment as potable water resources, Desal. Wat. Treat., 57 (2016) 7711–7720.
[8] W. Hao, M. Yang, K. Zhao, J. Tang, Dielectric measurements of fouling of nanofiltration membranes by sparingly soluble salts, J. Membr. Sci., 497 (2016) 339–347.
[9] J. Li, J. Liu, T. Yang, C. Xiao, Quantitative study of the effect of electromagnetic field on scale deposition on nanofiltration membranes via UTDR, Water Res., 41 (2007) 4595–4610.
[10] K. Xu, H. Q. Ren, L.L. Ding, J.J. Geng, T.T. Zhang, A review of membrane fouling in municipal secondary effluent reclamation, Environ. Sci. Pollut. Res., 20 (2013) 771–777.
[11] L. Llenas, G. Ribera, X. Martínez-Lladó, M. Rovira, J. de Pablo, Selection of nanofiltration membranes as pretreatment for scaling prevention in SWRO using real seawater, Desal. Wat. Treat., 51 (2013) 930–935.
[12] A.M. Farooque, M.Z. Alanazi, Sustainable performance of NF-SWRO pilot plant with low fouling NF membrane, Desal. Wat. Treat., 55 (2015) 2536–2542.
[13] H.H. Ou, L.H. Chiang Hsieh, A synergistic effect of sodium gluconate and 2-phosphonobutane-1,2,4-tricarboxylic acid on the inhibition of $CaCO_3$ scaling formation, Powder Technol., 302 (2016) 160–167.
[14] F. He, K.K. Sirkar, J. Gilron, Effects of antiscalants to mitigate membrane scaling by direct contact membrane distillation, J. Membr. Sci., 345 (2009) 53–58.
[15] R. Ketrane, B. Saidani, O. Gil, L. Leleyter, F. Baraud, Efficiency of five scale inhibitors on calcium carbonate precipitation from hard water: effect of temperature and concentration, Desalination, 249 (2009) 1397–1404.
[16] S. Sarkar, R.C. Smith, A.K. SenGupta, Reversible ion exchange-membrane (RIX-M) process for fouling free and energy efficient desalination of seawater, ACS Symp. Ser., 1078 (2011) 285–301.
[17] Z. Liu, S. Wang, L. Zhang, Z. Liu, Dynamic synergistic scale inhibition performance of IA/SAS/SHP copolymer with magnetic field and electrostatic field, Desalination, 362 (2015) 26–33.
[18] M. Rouina, H.R. Kariminia, S.A. Mousavi, E. Shahryari, Effect of electromagnetic field on membrane fouling in reverse osmosis process, Desalination, 395 (2016) 41–45.
[19] M.C. Chang, C.Y. Tai, Effect of the magnetic field on the growth rate of aragonite and the precipitation of CaCO3, Chem. Eng. J., 164 (2010) 1–9.

[20] C.Y. Tai, M.C. Chang, R.J. Shieh, T.G. Chen, Magnetic effects on crystal growth rate of calcite in a constant-composition environment, J. Cryst. Growth, 310 (2008) 3690–3697.
[21] C.Y. Tai, C.K. Wu, M.C. Chang, Effects of magnetic field on the crystallization of $CaCO_3$ using permanent magnets, Chem. Eng. Sci., 63 (2008) 5606–5612.
[22] S. Kobe, G. Dražić, A.C. Cefalas, E. Sarantopoulou, J. Stražišar, Nucleation and crystallization of $CaCO_3$ in applied magnetic fields, Cryst. Eng., 5 (2002) 243–253.
[23] S. Kobe, G. Draži, P.J. McGuiness, J. Stražišar, The influence of the magnetic field on the crystallisation form of calcium carbonate and the testing of a magnetic water-treatment device, J. Magn. Magn. Mater., 236 (2001) 71–76.
[24] F. Long, A. Zhu, X.L. Wang, W.P. Zhu, Membrane flux and $CaCO_3$ crystallization in the unstirred dead-end nanofiltration of magnetic solution, Desalination, 186 (2005) 243–254.
[25] F. Alimi, M. Tlili, M. Ben Amor, C. Gabrielli, G. Maurin, Influence of magnetic field on calcium carbonate precipitation, Desalination, 206 (2007) 163–168.
[26] L. Hołysz, E. Chibowski, A. Szcześ, Influence of impurity ions and magnetic field on the properties of freshly precipitated calcium carbonate, Water Res., 37 (2003) 3351–3360.
[27] T. Waly, M.D. Kennedy, G.J. Witkamp, G. Amy, J.C. Schippers, The role of inorganic ions in the calcium carbonate scaling of seawater reverse osmosis systems, Desalination, 284 (2012) 279–287.
[28] M. Gryta, The influence of magnetic water treatment on $CaCO_3$ scale formation in membrane distillation process, Sep. Purif. Technol., 80 (2011) 293–299.
[29] E. Chibowski, L. Hołysz, A. Szcześ, M. Chibowski, Precipitation of calcium carbonate from magnetically treated sodium carbonate solution, Colloid Surf., A, 225 (2003) 63–73.
[30] D.G. Schulze, J.B. Dixon, High gradient magnetic separation of iron oxides and other magnetic minerals from soil clays, Soil Sci. Soc. Am. J., 43 (1979) 793–799.
[31] S. Knez, C. Pohar, The magnetic field influence on the polymorph composition of $CaCO_3$ precipitated from carbonized aqueous solutions, J. Colloid Interface Sci., 281 (2005) 377–388.
[32] S. Phuntsho, F. Lotfi, S. Hong, D.L. Shaffer, M. Elimelech, H.K. Shon, Membrane scaling and flux decline during fertiliser-drawn forward osmosis desalination of brackish groundwater, Water Res., 57 (2014) 172–182.
[33] S. Shirazi, C.J. Lin, D. Chen, Inorganic fouling of pressure-driven membrane processes — a critical review, Desalination, 250 (2010) 236–248.
[34] S. Mattaraj, C. Jarusutthirak, C. Charoensuk, R. Jiraratananon, A combined pore blockage, osmotic pressure, and cake filtration model for crossflow nanofiltration of natural organic matter and inorganic salts, Desalination, 274 (2011) 182–191.
[35] D. Vogel, A. Simon, A.A. Alturki, B. Bilitewski, W. E. Price, L.D. Nghiem, Effects of fouling and scaling on the retention of trace organic contaminants by a nanofiltration membrane: the role of cake-enhanced concentration polarisation, Sep. Purif. Technol., 73 (2010) 256–263.
[36] C. Gabrielli, R. Jaouhari, G. Maurin, M. Keddam, Magnetic water treatment for scale prevention, Water Res., 35 (2001) 3249–3259.
[37] L.G. Bauer, Contact Nucleation of Magnesium Sulfate Heptahydrate in a Continuous MSMPR Crystallizer, Iowa State University, 1972.
[38] C.Y. Tai, J.F. Wu, R.W. Rousseau, Interfacial supersaturation, secondary nucleation, and crystal growth, J. Cryst. Growth, 116 (1992) 294–306.
[39] W.L. Ang, A.W. Mohammad, A. Benamor, N. Hilal, Hybrid coagulation–NF membrane processes for brackish water treatment: effect of pH and salt/calcium concentration, Desalination, 390 (2016) 25–32.
[40] T. Chen, A. Neville, M. Yuan, Calcium carbonate scale formation—assessing the initial stages of precipitation and deposition, J. Petrol. Sci. Eng., 46 (2005) 185–194.
[41] R.A. Dawe, Y. Zhang, Kinetics of calcium carbonate scaling using observations from glass micromodels, J. Petrol. Sci. Eng., 18 (1997) 179–187.
[42] N. Her, G. Amy, C. Jarusutthirak, Seasonal variations of nanofiltration (NF) foulants: identification and control, Desalination, 132 (2000) 143–161.
[43] C.Y. Tai, M.C. Chang, S.W. Yeh, Synergetic effects of temperature and magnetic field on the aragonite and calcite growth, Chem. Eng. Sci., 66 (2011) 1246–1253.
[44] N. Andritsos, M. Kontopoulou, A.J. Karabelas, P. G. Koutsoukos, Calcium carbonate deposit formation under isothermal conditions, Can. J. Chem. Eng., 74 (1996) 911–920.
[45] K. Nakamura, T. Orime, K. Matsumoto, Response of zeta potential to cake formation and pore blocking during the microfiltration of latex particles, J. Membr. Sci., 401–402 (2012) 274–281.